

**An electron diffraction study of a Ti-22 at. % Nb alloy containing unequal populations of the four variants of the  $\omega$ -phase**

The  $\omega$ -phase is a metastable phase which forms in Ti and Zr base transition-metal alloys and leads to mechanical embrittlement and an enhancement of superconducting critical currents of the alloys. For a recent review of the properties of the  $\omega$ -phase see Hickman [1]. There has been some inconsistency in the literature regarding the crystal structure of the  $\omega$ -phase. The results of studies using transmission electron microscopy and dark field techniques [2-5] support earlier X-ray results which indicated that the  $\omega$ -phase has a hexagonal crystal structure [6-10]. According to these results the hexagonal  $\omega$ -phase orients with respect to the body-centred-cubic  $\beta$ -phase in four different ways. The orientation of one of these variants is  $(0001)_\omega || (111)_\beta$  and  $[2\bar{1}\bar{1}0]_\omega || [\bar{1}\bar{1}0]_\beta$  where  $a_\omega = \sqrt{2}a_\beta$  and  $c_\omega = \sqrt{3}a_\beta/2$ . The remaining three variants are oriented in a similar manner with respect to the other three symmetrically equivalent  $\{111\}$  planes of the  $\beta$ -matrix. However, very recently X-ray results [11] have been purported to support other previous conclusions [12-14] that the  $\omega$ -phase has a body-centred-cubic structure. Generally the  $\omega$ -phase forms in equal proportions in the four possible

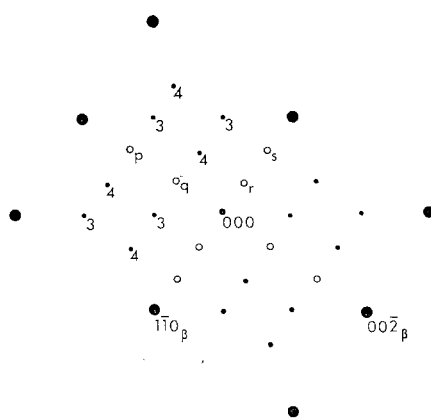
variants and this gives a diffraction pattern of spots with body centred-cubic symmetry. A study of symmetry alone can therefore lead to the erroneous conclusion that  $\omega$  is a cubic structure. However, unequal proportions of the four hexagonal variants have been observed in a Ti-13% Mo alloy [8] and displaced spots occur when the  $c/a$  ratio is not ideal [7]. In this present work a previously deformed specimen has been examined by transmission electron microscopy and shows very distinctly that different areas give different diffraction patterns. The only possible interpretation is that the  $\omega$ -phase is hexagonal with four variants which have unequal populations in various regions of the foil.

A Ti-22 at. % Nb alloy was prepared from iodide grade titanium and zone refined Nb using a standard arc melting technique. The arc melted alloy was homogenized at 1000°C for 72 h under a vacuum of  $1 \times 10^{-6}$  torr, cold rolled and then cut into strips measuring  $5.0 \times 1.3 \times 0.08$  cm<sup>3</sup>. The strip specimens were heated for 24 h at 1000°C followed by vacuum cooling to room temperature. The specimens were deformed by bending them backwards and forwards a number of times along the 5 cm length, the minimum radius of curvature of each bend being 1.3 cm. They were then aged under a vacuum for 40 h at 400°C.

Thin foils were obtained from the aged strips by chemically etching in a solution containing



(a)



(b)

Figure 1 (a)  $(110)_\beta$  transmission electron diffraction pattern obtained from a thick region of a Ti-22 at. % Nb alloy containing the  $\beta$ -matrix and  $\omega$ -precipitates. Unobscured diffraction spots containing in some cases contributions from the  $\omega$ -phase variants 1, 2, 3 and 4. ○ Diffraction spots produced by double diffraction

pattern obtained from a thick region of a Ti-22 at. % Nb alloy containing the  $\beta$ -matrix and  $\omega$ -precipitates. ●  $(110)_\beta$  diffraction spots from the  $\beta$ -phase containing in some cases contributions from the  $\omega$ -phase variants 1, 2, 3 and 4. ○ Diffraction spots produced by double diffraction between variants 3 and 4 of the  $\omega$ -phase.



Figure 2  $(110)_\beta$  transmission electron diffraction pattern illustrating the absence of the  $\omega$ -phase variant labelled 3.



Figure 3  $(110)_\beta$  transmission electron diffraction pattern illustrating the absence of the  $\omega$ -phase variants labelled 3 and 4.

equal parts water, sulphuric, hydrofluoric and nitric acids maintained at less than  $-10^\circ\text{C}$ . A Philips EM 300 electron microscope, operated at 100 kV, was used in this investigation.

Figs. 1, 2 and 3 show transmission electron diffraction patterns from the Ti-22 at. % Nb alloy prepared as described above, the electron beam being along the  $[110]$  direction of the  $\beta$ -matrix. These patterns were obtained from areas of decreasing foil thickness within a single  $\beta$ -phase grain. Fig. 1, representative of the thickest portion of the foil, is the kind of electron diffraction pattern usually observed from Ti base transition-metal alloys containing only the  $\beta$  and  $\omega$ -phases. It is this pattern which has been interpreted in terms of either  $\beta$  plus a hexagonal  $\omega$ -phase or  $\beta$  plus a body-centred-cubic  $\omega$ -phase. Comparison of the diffraction spots in the figures shows that the patterns have the same basic geometry but the intensities vary from one pattern to another. This effect is most easily explained in terms of different populations of four variants of a hexagonal  $\omega$ -phase which are oriented with respect to the  $\beta$ -matrix in the manner described earlier. For the purposes of the present letter only the geometry of the diffraction patterns is important, hence indexing in terms of Miller indices is not given in Fig. 1b. Such indexing already appears in the literature (see, for example, Sass [2]). When the electron beam is in the  $[110]$  direction of the  $\beta$ -matrix as is the case for Figs. 1 to 3 diffraction spots from two of the  $\omega$ -phase variants (labelled variants 1 and 2) are obscured by the matrix

spots. Some of the diffraction spots arising from the remaining two variants of the  $\omega$ -phase (labelled 3 and 4) are not obscured by matrix diffraction spots and it is these unobscured spots which may be used to account for the patterns shown. Reference to Fig. 1b and the diffraction patterns of Figs. 1a, 2 and 3 shows that Fig. 1a was produced by a region of the specimen containing approximately equal proportions of variants 3 and 4, Fig. 2 was obtained from a region which contained variant 4 but not variant 3 and Fig. 3 was obtained from a region which contained neither variant 3 nor variant 4. Sass [4] using tilting techniques showed that the diffraction spots p, q, r, s of Fig. 1 are not intrinsic spots of the  $\omega$ -phase but are due to double diffraction. This conclusion is supported by Figs. 2 and 3 where the geometries of the patterns are inappropriate for any of the spots p, q, r, s to be formed since the necessary double diffraction involves both variants 3 and 4, and accordingly these spots are not observed.

The buckling of foils can lead to changes in the intensities of spots in a diffraction pattern, however, foil buckling cannot account for the selective absences of spots from particular orientation variants as observed in the present experiments.

It has recently been suggested [11] that the  $\omega$ -phase has a body-centred-cubic structure with  $a_\omega \simeq 3a_\beta$  the cube axes being parallel to the corresponding axes of the body-centred-cubic  $\beta$ -phase. The symmetry of Fig. 2 is inconsistent with this explanation and it is for this reason that

Figs. 1-3 have been interpreted in terms of a hexagonal form of the  $\omega$ -phase.

The results of the present experiments raise the question as to the mechanism which leads to different populations of four  $\omega$ -phase variants. Electron diffraction patterns similar to that shown in Fig. 1 were obtained from all thick regions of the specimens. No evidence was obtained from these patterns to suggest that in these regions the population of the four  $\omega$ -phase variants was anisotropic. Figs. 2 and 3 were obtained from thin regions of the specimens where the  $\omega$ -phase variants show marked anisotropy in population. This indicates that the anisotropy may arise when an isotropic specimen (in the sense of equal population of the four  $\omega$ -phase variants) is thinned. Presumably preferential reversion of some variants of the  $\omega$ -phase to the parent  $\beta$ -phase occurs as a result of stress relaxation of the thin areas of the previously deformed foils.

None of the work published purporting to show that  $\omega$  has a cubic structure [11-14] is inconsistent with the hexagonal interpretation. The results of the present experiments are, however, inconsistent with the proposed cubic structure. Thus it must be concluded that the cubic interpretation of the omega phase structure is not valid.

### Acknowledgements

The authors are indebted to Mr S. Chinniah for photographic work and to the National Research Council of Canada for research funds.

### References

1. B. S. HICKMAN, *J. Mater. Sci.* **4** (1969) 554.

2. S. L. SASS, *Acta Metallurgica*, **17** (1969) 813.
3. M. J. BLACKBURN and J. C. WILLIAMS, *Trans. Met. Soc. AIME*, **242** (1968) 2461.
4. J. C. WILLIAMS and M. J. BLACKBURN, *Trans. ASM* **60** (1967) 373.
5. W. G. BRAMMER, JUN, and C. G. RHODES, *Phil. Mag.* **16** (1967) 477.
6. D. J. COMMETTO, G. L. HOUZE, JUN, and R. F. HEHEMANN, *Trans. Met. Soc. AIME*, **30** (1965) 233.
7. B. A. HATT and J. A. ROBERTS, *Acta Metallurgica* **8** (1960) 575.
8. J. M. SILCOCK, *Acta Metallurgica* **6** (1958) 481.
9. B. A. HATT, J. A. ROBERTS, and G. I. WILLIAMS, *Nature (Lond.)* **180** (1957) 1406.
10. J. M. SILCOCK, M. H. DAVIES, and H. K. HARDY, A Symposium, Monograph and Report Series, No. 18, p. 93 (London, Inst. of Metals, 1956).
11. E. U. LEE, *J. Appl. Cryst.* **3** (1970) 413.
12. C. HAMMOND, The Morphology of the Omega Phase, Presented at the International Conference on Titanium in London (May 23, 1968).
13. A. E. AUSTIN and J. R. DOIG, *Trans. Met. Soc. AIME* **209** (1957) 27.
14. W. M. PARRIS, C. M. SCHWARTZ, and P. D. FROST, Precipitation Hardening and Embrittlement of High-Strength Titanium Alloys, WADC Technical Report 54-355 (1955) Part II.
15. M. K. KOUL and J. F. BREEDIS, *Acta Metallurgica*, **18** (1970) 579.

Received 6 December 1971

and accepted 10 February 1972

T. S. LUHMAN

A. E. CURZON

Physics Department

Simon Fraser University

Burnaby 2

British Columbia, Canada

### Scanning electron microscope selected-area channelling patterns: dependence of area on rocking angle and working distance

In the selected-area channelling pattern (SACP) method in which the electron probe is made to rock about a "point" on the specimen surface, [1] the minimum selected-area size  $d$  is given in theory by  $d = \frac{1}{2}C_s\phi^3$ , where  $C_s$  is the spherical aberration coefficient of the final lens, and  $2\phi$  is the total angle of rock. The value of  $C_s$  depends on the working distance ( $WD$ ) of the final lens,

and so  $d$  depends on both  $2\phi$  and  $WD$ .

For many investigations, it is necessary for  $d$  to be small, e.g. in the 1 to 10  $\mu\text{m}$  range, and the conditions favouring this are small  $2\phi$  and small  $C_s$ . The value of  $2\phi$ , the angular width of the SACP, cannot generally be decreased much below 8 to 9° if useful patterns are to be obtained. However, the value of  $C_s$  can be decreased by using small values of  $WD$ , i.e. placing the specimen close to the final lens. It was for this reason that the SACP studies made during the last few years at the Westinghouse Research Laboratories [2, 3] were mostly performed with a